Mechanism and Machine Theory 165 (2021) 104430

Contents lists available at ScienceDirect

Mechanism and Machine Theory

journal homepage: www.elsevier.com/locate/mechmachtheory

Machine learning based nominal root stress calculation model for gears with a progressive curved path of contact

Uroš Urbas, Damijan Zorko*, Nikola Vukašinović

University of Ljubljana, Faculty of mechanical engineering, LECAD, Aškerčeva 6, 1000 Ljubljana, Slovenia

ARTICLE INFO

Article history:
Received 23 March 2021
Revised 8 June 2021
Accepted 8 June 2021

Keywords:
Machine learning
Nominal root stress
Gears
FEM
Random forest
AdaBoost

ABSTRACT

The study aims to investigate the possibility of employing machine learning models in the design of non-involute gears. Such a model would be useful for design calculations of non-standard gears, where there are no available guidelines. The aim is to create a decision-support model accompanying the Finite Element Method (FEM) simulations, from which the data for training was collected. Multiple models for numerical prediction were tested, i.e. linear regression, Support Vector Machine, K-nearest neighbour, neural network, AdaBoost, and random forest. The models were firstly validated with N-fold cross-validation. Further validation was done with new FEM simulations. The results from the simulations and the models were in good agreement. The best-performing ones were random forest and AdaBoost. Based on the validation results, a machine learning constructed model for calculating nominal root stress in gears with a progressive curved path of contact is proposed. The model can be used as an alternative to FEM simulations for determining the nominal root stress in real-time, and is able to calculate the stress for gears with different number of teeth, widths, modules, paths of contact, materials, and loads. Therefore, many combinations of gear geometries can be analysed and the most suitable can be chosen.

1. Introduction

Accurately calculating the tooth root stress is one of the most important tasks in gear design [1]. Gear performance is in many cases dependent on tooth root strength, since root cracks and final tooth breakage are a common failure type for steel [2,3] and polymer gears [4]. There are three main ways of determining the gear root stress, e.g.: analytical models, finite element method, and experimental tests. The development of analytical models for root strength control is presented in Lisle et al. [5]. Many decades of research have resulted in the international standard ISO 6336 [6], where methods for root strength control are given. An American standard, AGMA 2101-D04 [7], is also available. Differences between the two standards and their accuracy are discussed in Lisle et al. [5]. The main difference between these two standards is the method used for determining the critical section location at which the maximum root stress is calculated. Standard ISO 6336 uses the 30° tangent method, while the AGMA standard uses the Lewis parabola. It was found by Wen et al. [2] that both of these methods are less accurate at predicting the critical section location than the FEM method. Those authors presented an

* Corresponding author.
E-mail address: damijan.zorko@lecad.fs.uni-lj.si (D. Zorko).

https://doi.org/10.1016/j.mechmachtheory.2021.104430

Nomenclature

h_a	addendum height [mm]
Y_ε	contact ratio factor for root stress [/]
n	curvature parameter [/]
h_f	dedendum height [mm]
b	face width [mm]
Y_{Fa}	form factor [/]
Y_β	helix angle factor for root stress [/]
σ_{F0}	nominal root stress [MPa]
F_t	nominal tangential load, the transverse load tangential to the reference cylinder [N]
m_{n}	normal module [mm]
z	number of teeth of the gear [/]
α	pressure angle [°]
ROI	region of interest [/]
σ_F	root stress [MPa]
ρ_F	root fillet radius [mm]
Y_{Sa}	stress correction factor (notch effect) [/]
Y_{Z}	S-gears' shape factor for the root stress [/]
E	Young's modulus [MPa]

updated analytical model for a more accurate calculation of the maximum root stress. There have been efforts to extend the analytical models for other gear shapes [2,8,9]; however, the existing analytical models can only be used for involute gear geometry. Whereas, for the design of non-involute gears, FEM methods need to be employed.

FEM models and experimental test methods can achieve accurate results but they require large computational/financial resources and time. Gonzalez-Perez et al. [10] proposed a method to reduce the computational costs of a FEM model of meshing gears by using a multi-point constraint between different sections of gear geometry. Another possibility for reducing the FEM model is to simplify it into a 2D problem [11,12], where the geometry and boundary conditions allow for such simplification. The FEM model can include different materials [13,14], and gear shapes and forms [15], which cannot be calculated by analytical models, but it requires constructing the 3D CAD model with various calculation sections, a software licence, which can be expensive, and a non-trivial knowledge about the software. Moreover, it is a computationally difficult process. FEM models can also include gear geometric deviations (which can be accurately measured optically [16]) in stress calculations in order to take into account their effect on the stress concentration [17].

Experimental testing is also important, as its accuracy improves with better equipment. However, it has a higher requirement for test apparatus and the results cannot be acquired before the sample preparation. Equipment such as strain gauges can be used to determine the root stress caused by the load [5].

Product design usually involves a complicated multi-objective optimisation process [18,19], where many different design solutions can be obtained and must be evaluated. When optimising design parameters, it is impractical to simulate all the design combinations. FEM models, when properly built, are highly accurate and offer stress calculation for different gear shapes, however, they are computationally and labour intensive. Therefore, a decision-support system is needed. A surrogate model, which would provide similar results with less effort, is desired. Surrogate models are simple and fast tools that emulate the output of a more complex model in function of its inputs and parameters [20].

Analytical stress prediction models for involute gears are well established, therefore, this study aims to develop a nominal root stress prediction model for non-involute gear pairs with a progressively curved path of contact, so-called S-gears [21–23]. In an effort to leverage FEM's accuracy at a fraction of the computational cost, it is possible to create surrogate models. Reducing the order of the models is crucial for their usage in applications such as digital twins [24]. However, there is often a trade-off between the uncertainty interval or accuracy of the determined result and the ability to operate in real-time. The more parameters that are included in establishing a surrogate model, the better the model imitates the reference model and less information is lost. FEM models are theory rich, whereas Machine Learning (ML) models are data-rich and have the potential to learn from existing data sets to detect relationships not obvious to the theory-rich models. Moreover, the theory-rich FEM model can be used to generate a plentiful amount of data to form a data-rich model. This study proposes the development of a surrogate model through model reduction utilising ML. Other studies utilised FEM to train ML models for journal bearing fault diagnostics [25], and the design of metal-formed products [26]. Researchers in other studies used genetic algorithms to modify the tooth shape [27–29] or the hob tool shape [30] to achieve a more desirable tooth root stress condition. Furthermore, these studies require many iterative FEM simulations which are time expensive and would benefit from a surrogate model. Only one study [31] has been conducted on gear root stress analysis with ML thus far. In the study, geometric shape deviations of micro-gears, gathered by areal measurements, were incorporated in FEM analysis to calculate the tooth root stresses of the gears. The researchers employed artificial neural networks to relate the measured shape deviations of micro-gears with tooth root stresses on the respective teeth. The model used nine defined gear devia-

tions to determine the root stress. The same gear with different deviations was included in the model's learning, so it is only appropriate for the specified micro-gear under the same loads. Twelve gears pairs were considered in the model's learning and an ideal reference model with no deviations was also analysed and heavily weighted so that it comprised half of the training data. However, the model is only suitable for one specific geometry of the micro-gears, and not on gears with a different number of teeth, modules, paths of contacts, loads, widths, and material pairs.

Moreover, this is the first time machine learning models are used for stress prediction in gear design. The presented study proposes a method based on data mining, with the dataset taken from results presented by Zorko et al. [8], where a modified standard model for root stress calculation of non-involute gears with a progressively curved path of contact (S-gears) was proposed. The modified model presented by Zorko et al. [8][62] takes into account the effect of the special S-gear tooth shape and also the effect of load-induced teeth deflection, which can be significant for polymer gears. The authors conducted a comprehensive study on the effects affecting the tooth bending stress in S-gears. Complex, non-linear interrelations between gear geometry, material, and load were observed, making it difficult to develop a generalised stress prediction model. The proposed model can replace the labour, temporally, and computationally expensive FEM model, to facilitate simple and fast gear design calculations; however, it is valid only in the context of analysed parameters. Beyond the analysed parameters, the model can still be used as an approximation; however, for final validation, a FEM calculation is still necessary. In the presented study a novel application of machine learning methods for gear design was made, marking a step towards a faster and simpler design of non-involute gears. The developed approach, using a decision-support system, reduces the required number of iterative FEM simulations to obtain an optimal solution.

The rest of the article is structured as follows. Section 1.1 continues with the introduction of the used machine learning models. Section 2 describes the methodology of the study, including the analytical model for S-gear root stress calculation, data acquisition and description, data pre-processing, and the used machine learning model parameters. Section 3 displays the results of training the models, and the validation on new data. Lastly, the discussion about the usability of the proposed method is presented in Section 4, and the conclusion with the highlights of the study in Section 5.

1.1. Regression machine learning models

Artificial Intelligence and machine learning is regularly employed on gear applications, specifically for gear wear assessment [32], predicting contact characteristics [33], diagnosing gear faults [34–37], and predicting gear life [38,39], where ML is often used to identify defects submerged in strong meshing harmonics of many rotary components [40,41].

Machine learning models can be used for classification [32] or regression. Regression and classification both belong under supervised machine learning. They both use the same concept of employing known datasets to make predictions. The algorithms are used for mapping a function from the input to the output variable. The main difference between classification and regression is that the classification output variable is categorical, while for regression it is numerical. The numerical variable, therefore, can be an integer or a floating-point value. The opposite of supervised ML is unsupervised ML, which looks for patterns in a data set with no pre-existing labels. Models such as clustering and rule learning belong under unsupervised ML.

Numerical predictions or regressions can be performed with several models [42]; the most commonly used ones are neural network, AdaBoost, random forest, Support Vector Machine (SVM), k-Nearest Neighbours (kNN), and linear regression. There are other models, which are robust against noisy and fluctuating data and that can integrate expert knowledge, such as the Discrete Bayes Filter (DBF) [43]; however, such data is not present in this study.

A neural network is a computing system inspired by biological neural networks to solve problems in the same way as the human brain. The input layer is the first layer [33], which consists of a set of neurons representing input attributes. The inputs are then processed through the hidden layers. To handle non-linear, separable problems, typically at least one hidden layer is added [44]. Each transforms the values from the previous layer with a weighted linear summation followed by an activation function. The output layer receives the values from the last hidden layer and transforms them into output values. The backpropagation approach optimises the neuron weights to reduce the error of the prediction. The advantage of multi-layer perceptron is that it can learn non-linear models. A disadvantage is that they require tuning several parameters, as well as hyperparameters, such as batch size and the number of epochs. Neural networks were previously used for control applications [45], for crack fault detection in gearboxes [46], for the creation of a dynamics model [47], and for determining the optimal 3D printing parameters of polymer gears for achieving a longer lifecycle [48]. Convolutional neural networks are regularly used for deep learning [25] and image recognition of engineering parts [49].

A random forest model is built from decision trees [50]. Decision trees have a flowchart-like structure, where depending on the attribute values, the algorithm follows a specific branch and returns the output value. A statistical property, called information gain, determines which attribute to test at each node in the tree. The random forest model builds multiple decision trees, which take into account a random subset of attributes at each step [51]. The result of each tree is weighted equally when predicting the result. In regression, this means that the predictions at each tree are averaged. It is resistant to noise, outliers, and overfitting. It is not useful in the case of just a few attributes and can perform badly when there is a small percentage of relevant attributes. An often advised number of attributes for a single tree is $N = \log_2(\#\text{attributes})+1$. The random forest model was previously used for fault diagnosis in spur gears [52].

AdaBoost is an ensemble model that uses boosting and stands short for adaptive boosting. The difference from random forests is that AdaBoost uses multiple weak learners such as decision trees with only one node and two leaves, also called

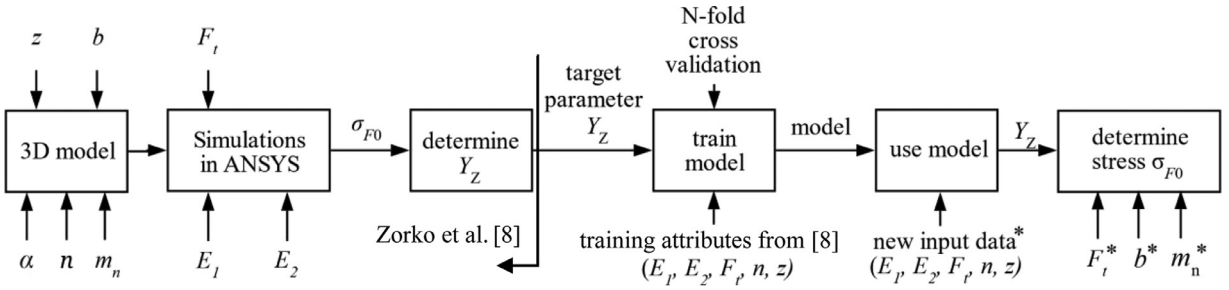

Fig. 1. Methodology used for the development of a machine learning based model for calculating tooth root stress.

stumps. The errors of the previous stump influence how the next stump is made. In the next iterations, it focuses on instances with the highest error, by increasing the weight of the instance. The model can reduce overall bias and variance, but can be sensitive to noise because the training can focus on bad data. The model was previously used in predicting sea surface temperatures [53].

SVM is a ML technique that separates the attribute space with a hyperplane, which maximises the margin between the instances of different classes. For regression tasks, the SVM performs a linear regression in a high-dimension attribute space. SVM was previously used for predicting contact characteristics for helical gears [33], and for a fault classification of gears [54].

The K-nearest neighbours algorithm searches for k closest training examples in attribute space and uses their average as a prediction value. The options that can be set are the number of neighbours that it considers, the weight of those neighbours, and the distance metric, which can, for example, be Euclidean or Manhattan. KNN was previously used for identifying different gear crack levels [55].

A linear regression model can be used as a baseline when comparing other models. It uses the least-squares error to optimally fit the data with a linear function.

2. Methodology

The research methodology is demonstrated with a flowchart in Fig. 1. The S-gear CAD models of the different gears were designed with an in-house developed Python software and then numerical simulations of gear pair meshing were conducted in ANSYS for different loads and material types. The simulation-calculated nominal root stress, which is the result of the simulation, was then used to determine the S-gear shape factor for root stress. The process is more clearly explained in a study by Zorko et al. [8][62]. The data was then used to train multiple machine learning models.

The N-fold cross-validation was used to split the data into training and testing datasets. The best models were determined with respect to the errors in the test dataset. New input data (marked with *) was then used on the models to predict the nominal root stress. The results were then compared with FEM simulations.

2.1. Analytical model for S-gear root stress calculation

The study is focused predominantly on polymer gears with a progressive curved path of contact. These gears outperform involute ones in some situations. The main identified advantages over involute gears include lower contact pressure at the start and end of meshing, lower sliding velocities, smaller losses due to less sliding in contact, and greater root thickness than involute gears of the same module [56]. Injection moulding is used to make the vast majority of mass-produced polymer gears. Since the shape of the gear profile has little impact on the expense of the injection moulding process, non-involute gear production may be economically justified.

There has been a lot of research on complex models and optimisation techniques [57] for involute gears. Models for polymer gear design [58,59] have also been presented, however, current methods and conversion models are only applicable to involute gears. The S-gear shape is non-standard; therefore, this study aims to develop a nominal root stress prediction model for non-involute gear pairs.

An analytical model for S-gears root strength control was proposed by Zorko [8]. The model is based on a large series of FEM simulations, which were used to characterize the effect of different S-gear parameters on the root stress of steel and polymer gears. The starting point of the study were the known standards for involute gears. Using DIN 3990:1987 Method C the nominal root stress σ_{F_0} can be calculated by the equation:

$$\sigma_{F_0} = Y_{F\alpha} \cdot Y_{S\alpha} \cdot Y_\varepsilon \cdot Y_\beta \cdot \frac{F_t}{b \cdot m_n} \tag{1}$$

The study is limited to spur gears hence $Y_\beta = 1$. Using known standards, the parameters $Y_{F\alpha}$, $Y_{S\alpha}$, and Y_ε are only defined for the involute gear shape. Therefore, a new parameter was introduced to consider the specific gear profile shape of gears with a progressive curved path of contact. The S-gear shape factor Y_Z [/] considers the effects of the tooth profile shape $Y_{F\alpha}$,

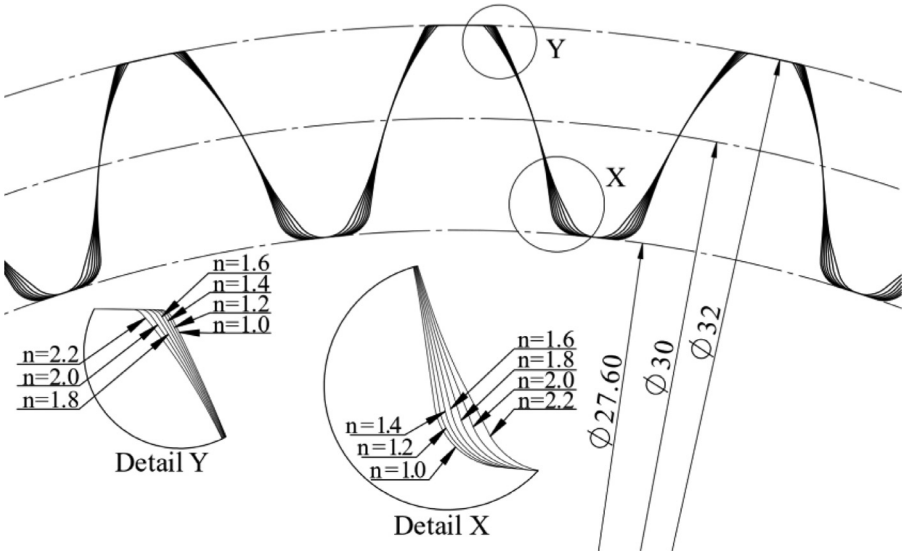

Fig. 2. Shape of the tooth dependent on z and n for a gear with 30 teeth and module 1 mm.

tooth root stress concentration $Y_{s\alpha}$, and transverse contact ratio Y_ε; so that $Y_Z = Y_{F\alpha} \cdot Y_{S\alpha} \cdot Y_\varepsilon$. The S-gear nominal root stress σ_{F_0} can be calculated by Eq. (2) [8]:

$$\sigma_{F_0} = Y_Z \cdot \frac{F_t}{b \cdot m_n} \tag{2}$$

where m_n [mm] is the normal module, b is the width of the gear, and F_t [N] is the tangential load on the reference diameter. The value of the parameter Y_Z is dependent on the curvature parameter (n [/]), the number of teeth (z [/]), and the actual contact ratio, which is dependent on the load on the tooth (F [N]) and the material combination of the materials used for the driving and the driven gear e.g. Young's modulus (E [MPa]). Complex nonlinear interrelations were found between these parameters. The shape factor Y_Z is, therefore, a function of f(E_1, E_2, F, n, z). E_1 is the Young's modulus of the driving gear and E_2 of the driven gear. Values of the shape factor Y_Z were determined by running many numerical simulations, making the model useful for a wide range of gear geometries and material combinations. The influence of the curvature parameter n and the number of teeth z on the S-gear profile shape is presented in Fig. 2. The effect of the curvature parameter n is analysed in the study [60]. As shown in the last stage of Fig. 1, once the parameter Y_Z is determined, Eq. (2) can be used to determine the nominal root stress σ_{F_0} for different gear widths and modules using. For that reason, the width and module do not need to be included in training of the ML model.

Once the specific gear profile shape of gears with a progressive curved path of contact is considered in the nominal root stress σ_{F_0} the real root stress σ_F can be calculated according to the known standards. The real root stress considers variations of output or input torque, internal dynamic effects, and uneven distribution of load in the transverse direction and over the face width.

2.2. Data acquisition

The data was acquired through a series of numerical simulations, which were run to characterize the shape factor Y_Z. A detailed description of the numerical modelling can be found in the work of Zorko et al. [8]. The non-linear dynamic FEM simulations were conducted using ANSYS software, where 2D models considering a plane stress state were used. Fig. 3 shows the FEM model of the gear pair; five teeth were modelled on the driving and the driven gear, and the root stress was analysed for the middle tooth, which was in mesh through all characteristic meshing points. The root failure occurs due to tensile stress in the tooth root, caused by the tangential load acting on the tooth. Accordingly, the highest tensile stress calculated during meshing was analysed in the study to determine the factor Y_Z. The radial load on the tooth and the frictional force imposed a compressive stress on the active flank side, which was considered by the FEM model. The compressive stress is also considered in the AGMA standard; however, it is neglected in the ISO and DIN standards. Mesh refinement was employed in the region of interest (ROI), where the element size was 0.016 mm. Mesh convergence was confirmed with the h-refinement method. The stress state during meshing of an S-gear pair is presented in Fig. 4. The region of interest was selected in a manner to observe the calculated bending stress in the entire root area (Fig. 4); in this way, the maximum root stress at the exact critical section could be determined and errors through the 30° tangent method or Lewis parabola were avoided [2]. The simulation includes large deflections and non-linear contacts between the meshing teeth. The domain discretization was achieved with quadratic order finite elements (PLANE183). CONTA172 elements on the

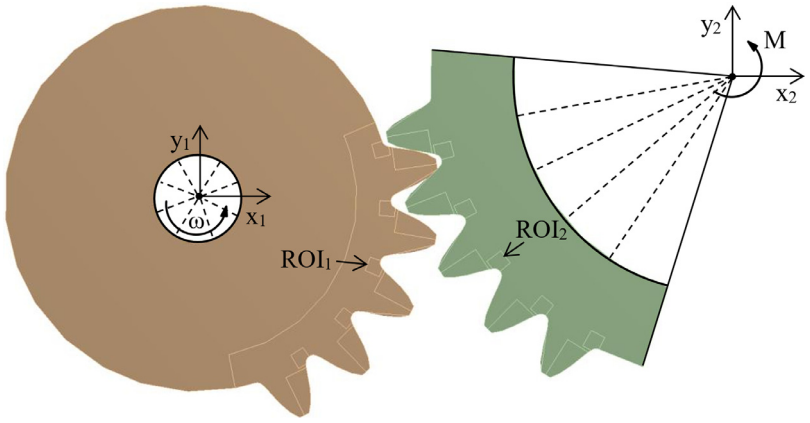

Fig. 3. The FEM model of a meshing gear pair.

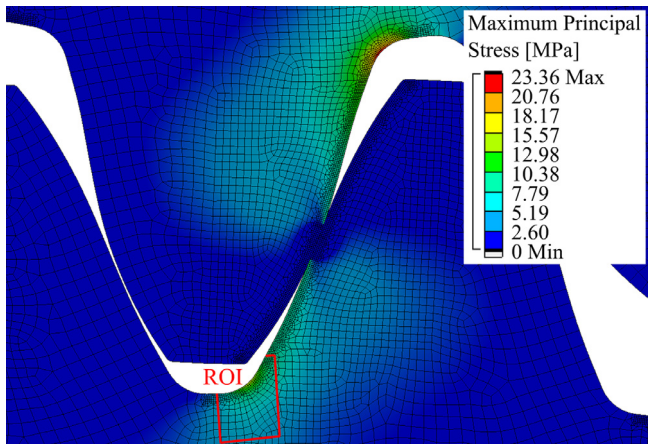

Fig. 4. The simulation-calculated stress state in the meshing gear-pair, with the indicated region of interest.

driving gear and TARGE169 elements on the driven gear were used to simulate the contact conditions. The mesh had an average composite quality of 0.96. As a result, a high-quality finite element mesh was used to determine the stress. The augmented Lagrange contact formulation algorithm was employed in the study. Fig. 3 displays the boundary and loading conditions of the analysis. The edge of the hole of the driving gear (left) was connected to a point in the origin of the coordinate system x_1, y_1 to only allow rotation around the z-axis. The edge of the hole has a prescribed rotation ω in the counter-clockwise direction. The driven (right) gear's inner and outer edges coloured in black were rigidly connected to a point in the origin of the coordinate system x_2, y_2 to allow rotation around the z-axis. The edges had a prescribed torque M in the counter-clockwise direction. The numerical model includes deformable geometry and considers the real contact ratio in the meshing of gears.

Different combinations of driving and driven gear were simulated. The first set of data consisted of 420 simulations, where the driving gear always had 20 teeth and the driven one had 20, 30, 50, 75, and 100 teeth. In such a way, the influence of the number of teeth on the tooth shape and the corresponding simulation-calculated root stress was considered. The initial pressure angle was set to $\alpha_{P0} = 20^{\circ}$, addendum height to $h_a = 1 \cdot$ m, dedendum height to $h_f = 1.2 \cdot$ m, and root fillet radius to $\rho_F =$ 0.3 mm. The shape of the S-gear profile is also dependent on the value of the curvature parameter n, wherefore geometries with curvature parameters ranging from $n = 1.0$ up to $n = 2.2$ were analysed. Linear elastic material was considered in all cases. As was confirmed in the work of Černe et al. [61], such an assumption is adequate when simulating polymer gear pair meshing. The Young's modulus ranged from 2800 to 200,000 MPa for the driven and the driving gear. The load ranged from 40 to 160 N with a 40 N increment. This formed the basis of the training data on which the models were trained in the first iteration.

The models were then used for gear root stress assessment of gear pairs used in real-life applications. When new design calculations outside the training data were needed, these simulations were included in the dataset, on which the final models were trained. The number of added simulation data to the training dataset was 36. These new simulations expanded the load range from 200 to 1000 N, and included gears with 17 teeth. Due to the smaller training data set in that area, it is expected that the accuracy in the expanded region is inferior.

Table 1
Example of the attributes and target parameter.

E_1 [MPa]	E_2 [MPa]	F_t [N]	n [/]	z [/]	Y_z [/]
200,000	200,000	160	1	20	4.14262
2800	3500	40	2	20	3.27105
200,000	3500	40	2	75	2.08905
200,000	3500	80	2.2	75	1.81095
2800	3500	120	1	75	1.6941
200,000	2800	160	1	50	2.26897
...	...	...	...	...	...

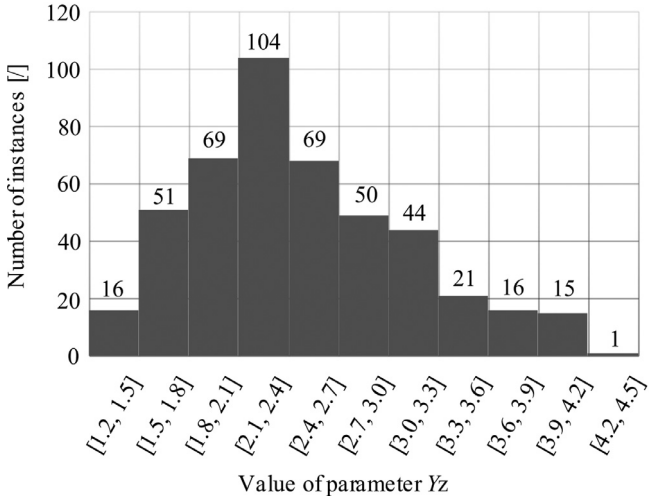

Fig. 5. Distribution of target value in the dataset.

2.3. Data description

In this research, the data from 456 simulations was used. Each of them represents an item in the item set. There are 5 attributes in each item, which are E_1, E_2, F_t, n, z. The attributes and the resulting parameter Y_z are all numerical values. There are no missing values. Table 1 shows an example of the attributes and the target variable used in the project. The simulations were done with material combinations of steel/steel with 2 different loads, steel/POM with 3 loads, steel/PA66 with 3 loads, and POM/PA66 with 4 loads. PA66 has a Young's modulus of 3500 MPa, POM 2800 MPa, and steel 200,000 MPa. The combination of z and n was changed during the same loads. The training attributes do not include the gear width, because the training was based on 6 mm-wide gears, with normal module $m_n = 1$. However, the gears can be of different widths and modules, as both parameters are considered in Eq. (2) for calculating the gear nominal root stress.

The distribution of the target variable Y_z in the training dataset is shown in Fig. 5.

2.4. Data pre-processing and evaluation criteria

The data of the 456 FEM simulations needed to be pre-processed to be used in training of the ML models. To prepare the data, the shape factor Y_Z needed to be calculated by expressing the shape factor from Eq. (2).

The attribute score was performed on the data, which is an assessment of the usefulness of the attribute for prediction of the target variable. The scoring method RReliefF is a modified classification scoring method, which can be used for regression. The results of the scoring method show that the most useful attributes in the dataset are attributes z and n, followed by F, and lastly E_1 and E_2.

The evaluation criteria used were the mean square error – MSE, root mean square error – RMSE, mean absolute error – MAE, and the correlation coefficient – R^2, which are normally used for determining the performance of the models used for numerical prediction.

2.5. Machine learning model parameters

Numerical prediction can be done with several models. The structure used for training and using the models is depicted in Fig. 6. The original dataset was used for training the different ML models. In the test and score function, the cross-validation method was used on the data. The number of folds was set to 20, which splits the data into 20 blocks, trains the

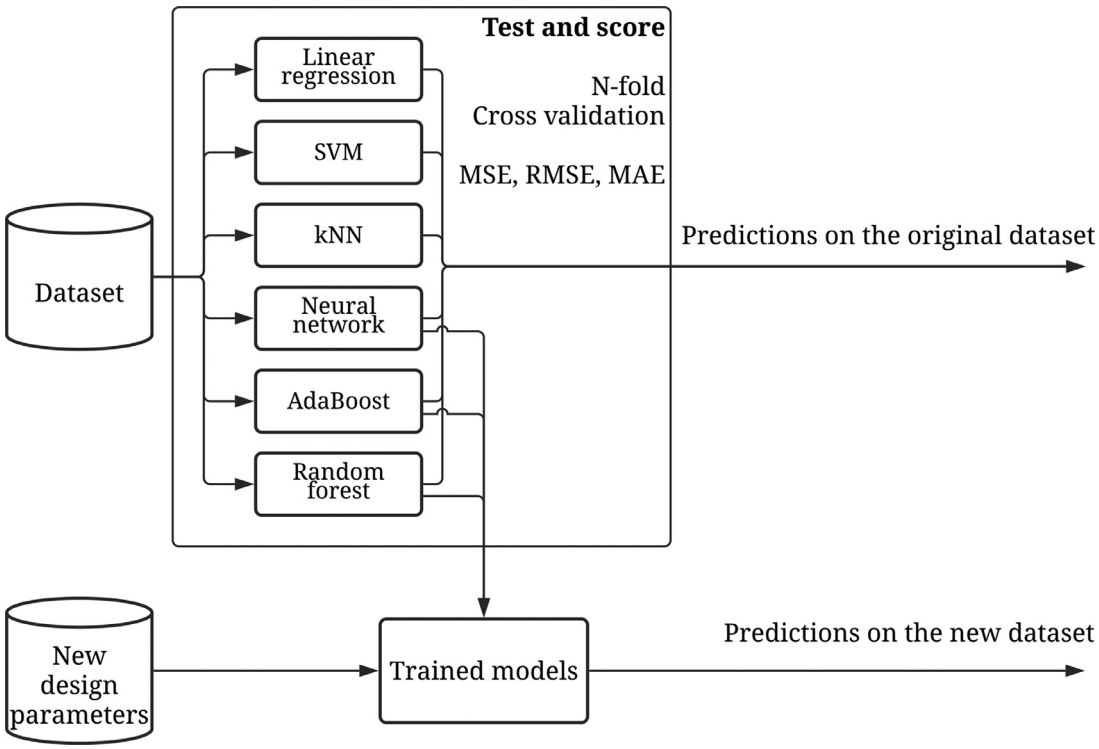

Fig. 6. Workflow of training and using the model.

model with 19 blocks, and tests the data with 1 block. Each block is used once for testing. By averaging the deviations on the predictions on the original dataset for 20 folds, the MSE, RMSE, MAE, and R^2 can be determined. The trained models are then able to predict the parameter Y_z on completely new design parameters.

The neural network consisted of a multi-layer perceptron algorithm with backpropagation. The number of neurons in the hidden layers was set to 270. ReLu (rectified linear unit function) was the used activation function. It has good gradient propagation and efficient computation. The function sets all of the negative values to zero and uses the identity function for the rest of the values. This simulates how a real neuron works. The solver for weight optimisation was *L-BFGS-B*, which starts with an initial estimate of the optimal values and then proceeds iteratively to refine the estimate with a sequence of better estimates. The regularisation penalty parameter was set to α=0.0001. The maximal number of iterations was 180. The solver iterates until the convergence determined by the tolerance value, or to this number of iterations. The tolerance for the optimisation was set to $1 \cdot 10^{-4}$. When the loss function does not improve by at least that value, the training stops. When using other solvers like *SGD* and *ADAM*, more parameters need to be set. However, for small datasets, the *L-BFGS-B* can converge faster and perform better. The number of neurons and the active function was likewise optimized.

The random forest model builds multiple trees, with a set number of random attributes. The model built 80 decision trees. Using full-grown trees seldom costs much and results in one less tuning parameter [51]; such an approach was accordingly used. Taking the equation for determining the number of attributes at random split into consideration $N = \log_2(\#\text{attributes})+1$, the number of attributes for training the trees was 3.

The number of estimators or trees for the AdaBoost model was 45 and a square regression loss function was used. The learning rate was set to 0.99995.

The SVM used a Radial Basis Function (RBF) kernel. The regression loss ε was set to 0.1 and the penalty term was set to 0.95. The kNN used 3 neighbours with the Euclidean distance and uniform weighting. The linear regression model used no regularisation.

3. Results

Multiple ML models were tested. The results for the evaluation criteria of all the models are displayed in Table 2.

The training time for each of the linear regression, SVM, and kNN models was 0.7 s, the time to train the AdaBoost and random forest was 1.6 s, whereas the neural network took 8.5 s to train. The computational complexity differs for the models. When dealing with a larger number of items in the training dataset, this can have an influence on the time. The complexity of machine learning algorithms is hard to determine, nevertheless, the linear regression has a linear, random

Table 2
Evaluation results for the N-fold cross-validation.

Model	MSE	RMSE	MAE	R^2
Random forest	0.026	0.161	0.078	0.939
AdaBoost	0.033	0.182	0.094	0.921
Neural network	0.039	0.198	0.088	0.906
SVM	0.050	0.223	0.135	0.882
kNN	0.061	0.248	0.147	0.854
Linear regression	0.143	0.378	0.304	0.661

Table 3
New data for prediction.

	E_1 [MPa]	E_2 [MPa]	F_t [N]	n [/]	z [/]	m [mm]	b [mm]
1	200,000	10,000	40	2.2	20	1	6
2	200,000	10,000	40	1	30	1	6
3	200,000	10,000	40	2.2	30	1	6
4	200,000	10,000	80	1	30	1	6
5	200,000	10,000	80	2.2	30	1	6
6	200,000	10,000	160	2.2	20	1	6
7	200,000	10,000	160	2.2	75	1	6
8	200,000	10,000	160	1	100	1	6
9	200,000	200,000	500	2.1	17	0.8	4
10	200,000	2800	80	2.1	73	0.8	5
11	200,000	3500	100	2.1	73	0.8	5
12	3500	2800	60	2.1	17	0.8	4

forest a quadratic and SVM a cubic complexity. However, the training time of the models does not differ significantly on the training data of this scale and is not limiting the use of any of the trained models.

The linear regression model is the only one that can be expressed in the form of an equation. However, according to the evaluation criteria, it was the least accurate. The model returns coefficients for each parameter and the Eq. (3) for determining the target value can be written:

$$Y_Z = 3.361 + E_1 \cdot 2.614 \cdot 10^{-6} + E_2 \cdot 1.949 \cdot 10^{-6} + \mathrm{F}_t \cdot \left(-5.023 \cdot 10^{-4}\right) + n \cdot (-0.268) + z \cdot (-0.015) \tag{3}$$

The coefficients for Young's modulus of both materials are small, because the inputs to the model are in MPa and are large numbers, as can be seen in Table 1. The weight values do not necessarily reflect the importance of the attribute, which would be the case if the input values were normalised. Otherwise, the normalisation has no impact on the results.

According to the evaluation results, the best-performing models were the random forest, AdaBoost, and neural network. All of them achieve a correlation coefficient of higher than 0.9. However, these are the results for N-fold cross-validation data. When predicting on new input data, the errors can differ slightly.

The best performing model is the random forest, which predicts the target value with an ensemble of decision trees. The decision trees can be shown with Pythagorean Forest visualisation. It displays them as Pythagorean trees, each visualization pertaining to one randomly constructed tree. The best tree is the one with the shortest and most strongly coloured branches. This means that few attributes split the branches well. Pythagorean visualisation is fit for showing big trees and their structures. Fig. 7 shows the 45th decision tree at depth level ten. The size of the edges of the squares represents the number of data instances that are present at that point. The colour of the squares presents the target value, which corresponds to the adjacent legend. The figure presents how the algorithm decides the value of the target parameter. The presented node I. in Fig. 7 contains 22 samples with a mean value of 2.893 and standard deviation of 0.234. The samples have the following attributes: $E_1 > 101{,}400$ MPa, $E_2 > 101{,}400$ MPa, $n \leq 1.925$, and the number of teeth (z) is between 25.5 and 40. The next split is by the tangential load F_t, to values bigger and smaller than 60 N. The result is determined by the average of the separate target values of the decision trees.

3.1. Validation on new data

The models were used for predicting the parameter Y_z and consequently the stress on new gear pair designs. Twelve new simulations were made and compared to the results of the trained machine learning models. The new data for prediction is shown in Table 3. The material with Young's modulus of 10,000 MPa is a composite of polymer and glass fibre. The tested material combinations are commonly used in practice.

The results are shown and compared in Fig. 8 and Fig. 9. The numbers on the x-axis represent each new simulation result as shown in Table 3. Fig. 8 shows a comparison of the nominal root stress determined by the FEM simulations and by the ML models. For a better presentation, Fig. 9 presents the relative deviations of the models, compared to the FEM simulations.

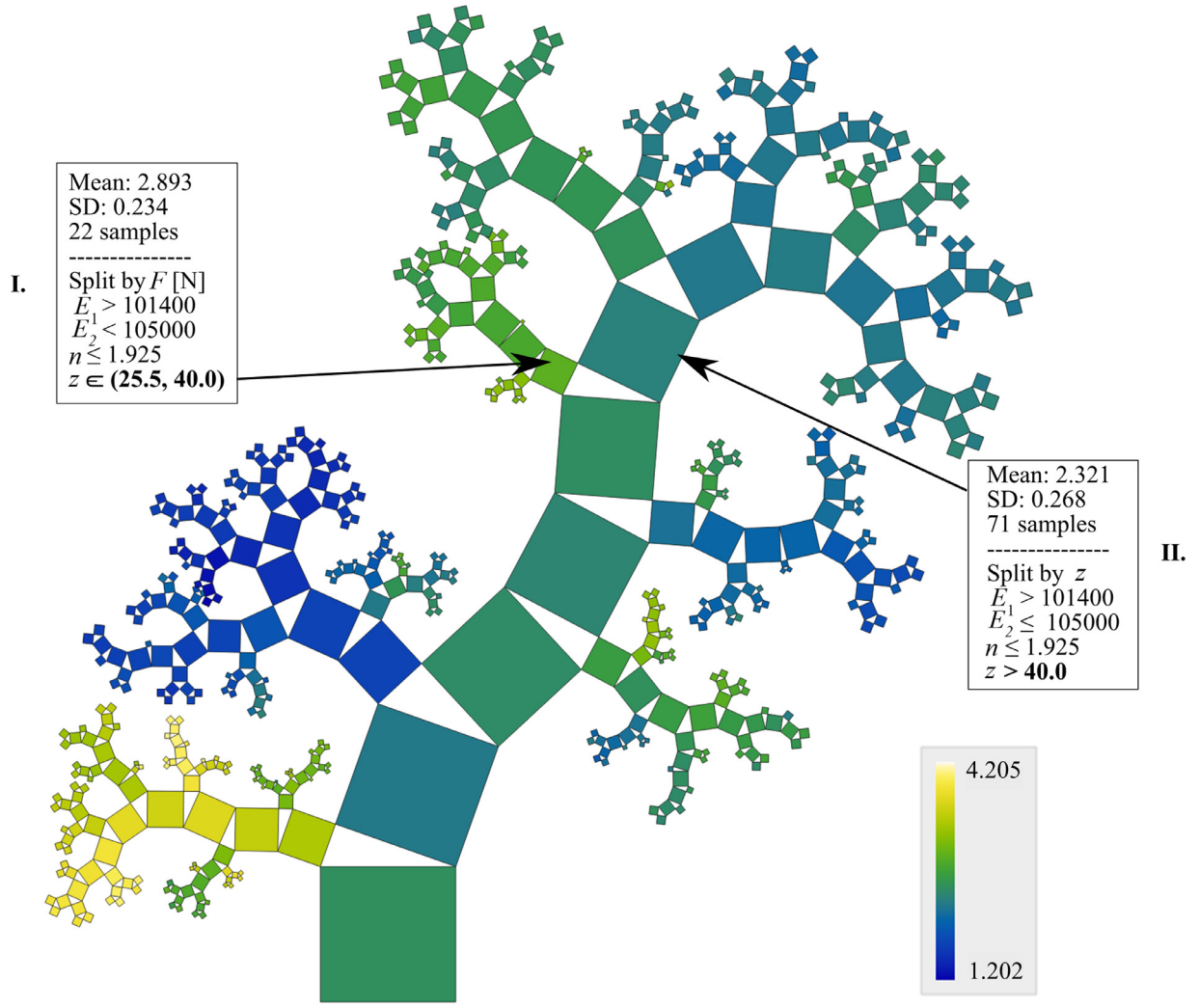

Fig. 7. Pythagorean forest visualization of the 45th tree at depth level 10.

The simulation-calculated stress is in good agreement with the model-calculated stress. The trained models can serve as a quick evaluation of the gear geometries, as can be seen in Fig. 8. The results are additionally presented in Fig. 9, which shows the relative deviation of the ML models compared to the simulation results. The AdaBoost and random forest models are again the best-performing ones. All of the results are within a 10% deviation. There are some higher deviations in the fourth and the twelfth case as there were fewer training data with similar attribute values, and the model is less capable of accurately predicting with those input values. The cases from the first to the eighth one were done on data, which is similar to the training data and only up to 2 attributes had different values than the training cases. The cases from the ninth to the twelfth one had more parameters that are different than the training cases.

The average relative deviation of the AdaBoost and random forest to the FEM method is 3.4% for both models. The standard deviation of the relative deviations is 4.1% for the AdaBoost model and 4.2% for the random forest.

4. Discussion

The traditional and new process of designing the non-involute gear pairs are illustrated in Fig. 10 and Fig. 11 respectively. There are N gear pair design combinations all depending on the required torque, rotational speed, desired life span, and working conditions. The traditional method requires a FEM simulation for each of the designs, which is resource and time-consuming. Due to practical reasons, only m-designs are tested with FEM simulations, where m<N. If the stress value is satisfactory the design moves on to the next step, where the acceptable designs are compared and the final one is chosen. The new method, however, considers all of the design variants; m = N. The ML model evaluates all of the input design

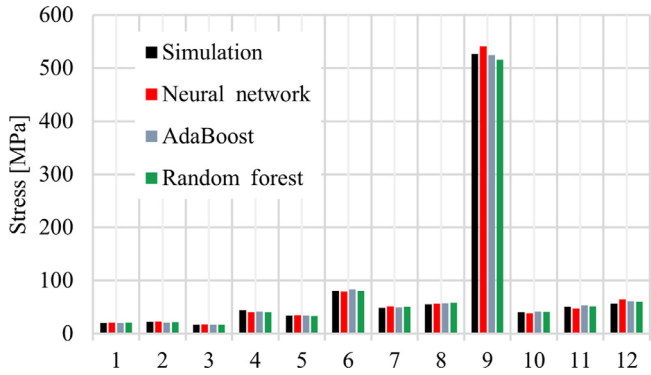

Fig. 8. Results of nominal root stress prediction and comparison to FEM simulation.

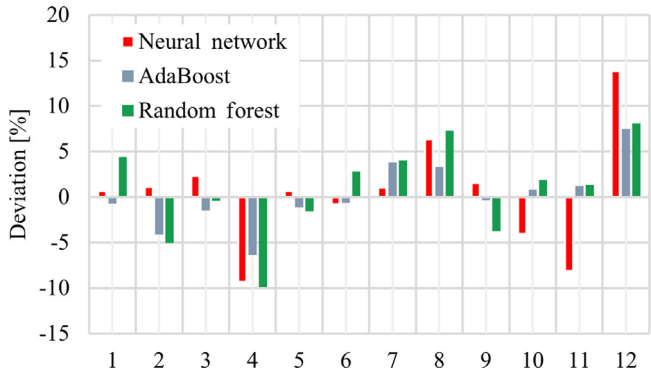

Fig. 9. Relative deviation of the ML models compared to the FEM simulation results.

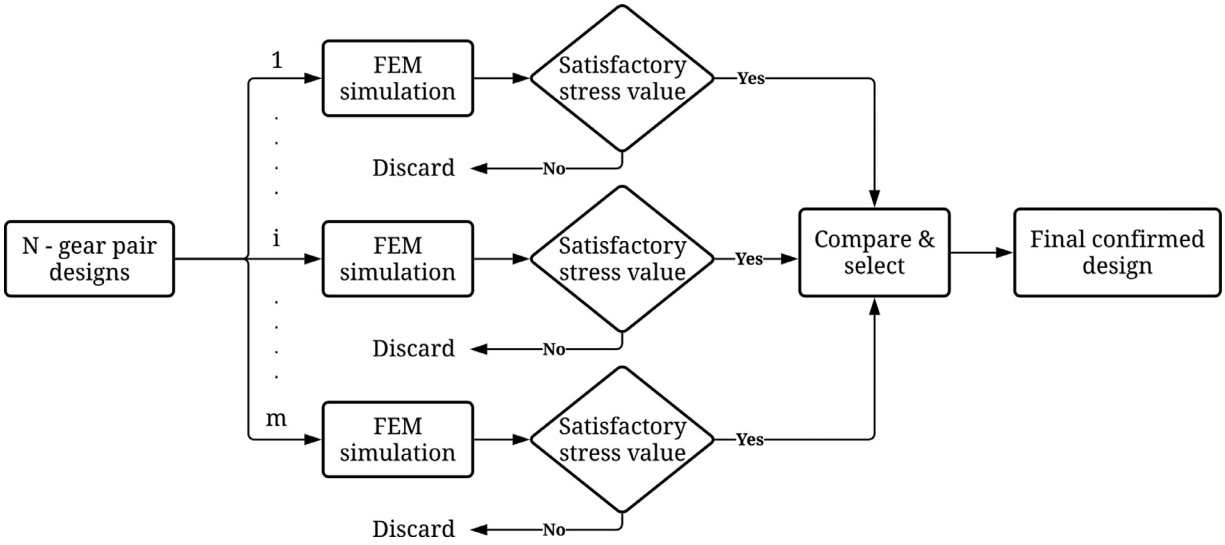

Fig. 10. Workflow of the traditional method.

parameter combinations, which are available in the design space to solve a problem. Only the best performing design is validated using FEM. If the results fit, the design is confirmed. If not, the instance is added to the training set.

The construction of the model for each design and meshing is a prerequisite to the simulation. This can normally take around 45 min. The time required to solve the simulation depends on the mesh density and whether it is simulated in 2D or 3D. Usually, when simulating the meshing of the two gears, at least 30 separate static simulations are required to calculate stress in several different meshing points, which can take an additional 15 min. An average of 5 different geometries are simulated when designing the gear pair. The method with the ML model, however, only includes the final validation of the

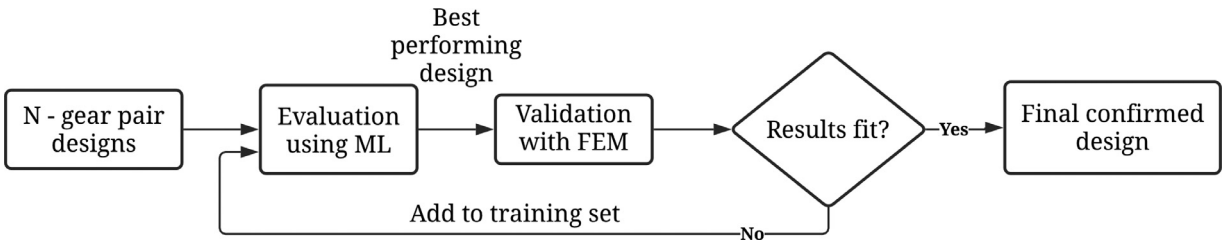

Fig. 11. Workflow of using the new support-decision model.

design with the FEM tool. The time needed to achieve the first step in choosing the optimal geometry with the ML model is negligible. Therefore, the proposed method enables an average of fivefold faster times to obtain and validate the final design.

The machine learning models deliver good results for the trained conditions. However, extreme care must be taken to ensure that the models are trained for all relevant settings and that the inputs are within the training data scope, as extrapolation can lead to substantial errors.

The problem that arises with using machine learning models to create a substitute model is the explainability of the model. With an understanding of the finite element method, a FEM model's output can be understood and explained. It is much more difficult to explain a neural network, which is a black-box model. AdaBoost and the random forest model are somewhat more explainable with viewing the development of the trees. Amongst the used models, linear regression is the most understandable, as the output of the training are fixed weights that are then used for the calculation. It does, however, result in the highest error.

Multiple models were tested and AdaBoost and random forest were the two best-performing models. However, the model that turned out the best might be best by chance and it can possibly over-fit the data. AdaBoost and random forest are similar models, where AdaBoost aims to upgrade the random forest model with boosting. It also requires data without noise, which this study had.

Furthermore, neural networks are better at problems with much more data, e.g. image and video processing, and 2D and 3D grids. Random forests are better with pre-processed data, where attributes are already extracted. However, when the dimensionality (number of attributes) is very high with respect to the number of training samples, a regularized linear regression or SVM could perform better than random forest.

The proposed machine learning model enables simple and fast gear design calculations. A large set of different gear geometries can be analysed much more quickly than by using FEM methods. Therefore, the final confirmed gear design for the desired application can be found more quickly. However, for a final validation, it is recommended to employ an FEM simulation.

From the calculated deviations it is possible to conclude that the model enables a good assessment of non-involute gear nominal root stress. Howbeit, changes to the pressure angle, root fillet radius, or addendum/dedendum coefficient will result in a changed gear profile shape. In that event, the values given by the model may not be valid.

The trained models are available on the Mendeley data repository in the pkcl format. They can be downloaded and loaded in Python. The user inputs the curvature parameter n, the number of teeth z, the load on the tooth F_t, and Young's modulus E of the materials used for the driving and the driven gear. The model then outputs the S-gear shape factor for root stress Y_Z. Using Eq. (2), the nominal root stress σ_{F_0} for the given design can be determined, by multiplying the shape factor Y_Z with the load F_t and dividing by the width of the gear b and normal module m_n.

5. Conclusion

A machine learning method for predicting the value of parameter Y_Z and consequently the nominal gear root stress was proposed. This is the first time that machine learning models have been used in gear design calculations. The method involves training the machine learning models from the data gathered from finite element simulations.

- Multiple models were trained, and the best-performing ones were random forest and AdaBoost, which achieved an average relative deviation of 3.4% compared to the reference FEM method. The resulting models were then validated on new data and the nominal root stress was calculated from the target parameter Y_Z, which is a function of attributes E_1, E_2, F_t, n, and z.
- The developed model enables a much simpler and faster technique of determining and assessing gear root stress in gear design. It can be used to calculate the nominal root stress for gears with different number of teeth, widths, modules, paths of contact, materials, and loads.
- It is especially appropriate for calculations in the design of nonstandard gear geometries.

Further work should be done on training the models with more data for different materials, loads, and gear shapes.

The models permit real-time computing and could be used within a larger digital twin if it also included data from sensors or measured deviations of the geometry of the gear. The prediction could then focus on lifetime assessments.

Data accessibility

The raw data that was used as the basis of the training data is accessible on the Mendeley data repository: https://data.mendeley.com/datasets/882g6st7f9/draft?a=21662788-4892-427c-b27b-26f8894b6d38. The processed training, and test data, along with the ML models for the random forest, AdaBoost and neural network are accessible on the Mendeley data repository: https://data.mendeley.com/datasets/sp3hcpmczn/draft?a=076c8c2c-7e71-461a-b352-6165b0e166b9.

Declaration of Competing Interest

The authors declare that they have no known competing financial interests or personal relationships that could have appeared to influence the work reported in this paper.

Acknowledgements

This research was financed partly by the MAPgears project (the project is co-financed by the Republic of Slovenia and the European Union under the European Regional Development Fund, contract no. C3330–18–952014) and partly by the Slovenian Research Agency (MR No. 51899).

Supplementary materials

Supplementary material associated with this article can be found, in the online version, at doi:10.1016/j.mechmachtheory.2021.104430.

References

[1] L. Bonaiti, A.B.M. Bayoumi, F. Concli, F. Rosa, C. Gorla, Gear root bending strength: a comparison between Single Tooth Bending Fatigue Tests and meshing gears, J. Mech. Des. (2021) 1–17, doi:10.1115/1.4050560.
[2] Q. Wen, Q. Du, X. Zhai, A new analytical model to calculate the maximum tooth root stress and critical section location of spur gear, Mech. Mach. Theory. 128 (2018) 275–286, doi:10.1016/j.mechmachtheory.2018.05.012.
[3] O. Doğan, C. Yuce, F. Karpat, Effects of rim thickness and drive side pressure angle on gear tooth root stress and fatigue crack propagation life, Eng. Fail. Anal. 122 (2021) 105260, doi:10.1016/j.engfailanal.2021.105260.
[4] C. Hasl, H. Liu, P. Oster, T. Tobie, K. Stahl, Forschungsstelle fuer Zahnraeder und Getriebebau (Gear Research Centre), Method for calculating the tooth root stress of plastic spur gears meshing with steel gears under consideration of deflection-induced load sharing, Mech. Mach. Theory. 111 (2017) 152–163, doi:10.1016/j.mechmachtheory.2017.01.015.
[5] T.J. Lisle, B.A. Shaw, R.C. Frazer, External spur gear root bending stress: a comparison of ISO 6336:2006, AGMA 2101-D04, ANSYS finite element analysis and strain gauge techniques, Mech. Mach. Theory. 111 (2017) 1–9, doi:10.1016/j.mechmachtheory.2017.01.006.
[6] ISO 6336: Calculation of load capacity of spur and helical gears, Parts 1-6, International standard, (2006).
[7] ANSI/AGMA 2101-D04: Fundamental rating factors and calculation methods for Involute Spur and Helical Gear Teeth (Metric Edition), (2016).
[8] D. Zorko, B. Černe, J. Duhovnik, R. Žavbi, J. Tavčar, Conversion Model for the Design of Steel and Polymer S-Gears, American Society of Mechanical Engineers Digital Collection, 2019, doi:10.1115/DETC2019-97817.
[9] T. Jabbour, G. Asmar, Tooth stress calculation of metal spur and helical gears, Mech. Mach. Theory. 92 (2015) 375–390, doi:10.1016/j.mechmachtheory.2015.06.003.
[10] I. Gonzalez-Perez, A. Fuentes-Aznar, Implementation of a finite element model for stress analysis of gear drives based on multi-point constraints, Mech. Mach. Theory. 117 (2017) 35–47, doi:10.1016/j.mechmachtheory.2017.07.005.
[11] D. Zorko, I. Demšar, J. Tavčar, An investigation on the potential of bio-based polymers for use in polymer gear transmissions, Polym. Test. (2020) 106994, doi:10.1016/j.polymertesting.2020.106994.
[12] V. Roda-Casanova, F. Sanchez-Marin, Development of a multiblock procedure for automated generation of two-dimensional quadrilateral meshes of gear drives, Mech. Mach. Theory. 143 (2020) 103631, doi:10.1016/j.mechmachtheory.2019.103631.
[13] T.G. Yılmaz, O. Doğan, F. Karpat, A comparative numerical study of forged bi-metal gears: bending strength and dynamic response, Mech. Mach. Theory. 141 (2019) 117–135, doi:10.1016/j.mechmachtheory.2019.07.007.
[14] F. Karpat, T.G. Yılmaz, O. Doğan, O.C. Kalay, Stress and mesh stiffness evaluation of bimaterial spur gears, in: american Society of Mechanical Engineers digital collection, 2020. https://doi.org/10.1115/IMECE2019-11554.
[15] T.G. Yılmaz, O. Doğan, C. Yüce, F. Karpat, Improvement of Loading Capacity of Internal Spur Gear With Using Asymmetric Trochoid Profile, American Society of Mechanical Engineers Digital Collection, 2018, doi:10.1115/IMECE2017-71009.
[16] U. Urbas, D. Zorko, B. Černe, J. Tavčar, N. Vukašinović, A method for enhanced polymer spur gear inspection based on 3D optical metrology, Measurement 169 (2021) 108584, doi:10.1016/j.measurement.2020.108584.
[17] B. Haefner, G. Lanza, Function-oriented measurements and uncertainty evaluation of micro-gears for lifetime prognosis, CIRP Ann 66 (2017) 475–478, doi:10.1016/j.cirp.2017.04.065.
[18] H.-.Z. Huang, Y.-.K. Gu, X. Du, An interactive fuzzy multi-objective optimization method for engineering design, Eng. Appl. Artif. Intell. 19 (2006) 451–460, doi:10.1016/j.engappai.2005.12.001.
[19] S. Belarhzal, K. Daoudi, E.M. Boudi, A. Bachir, S. Elmoumen, A multiobjective optimization analysis of spur gear pair: the profile shift factor effect on structure design and efficiency, Math. Probl. Eng. 2021 (2021) e8873769, doi:10.1155/2021/8873769.
[20] M.J. Asher, B.F.W. Croke, A.J. Jakeman, L.J.M. Peeters, A review of surrogate models and their application to groundwater modeling, Water Resour. Res. 51 (2015) 5957–5973, doi:10.1002/2015WR016967.
[21] Jože Hlebanja, Gorazd Hlebanja, Spur and helical gears with a basic rack profile with straight line y=k.x and parabola y=m.a.(1-(1-x/m)n), Slovenian National Patent nr. 20032, 2000.
[22] B. Trobentar, S. Kulovec, G. Hlebanja, S. Glodež, Experimental failure analysis of S-polymer gears, Eng. Fail. Anal. 111 (2020) 104496, doi:10.1016/j.engfailanal.2020.104496.

[23] Jože Hlebanja, Ivan Okorn, Charakteristische Eigenschaften von Zahnrädern mit stetig gekrümmter Eingriffslinie, Sonderdruck aus antriebstechnik 38 (1999).
[24] D. Hartmann, M. Herz, U. Wever, Model Order Reduction a Key Technology for Digital Twins, in: reduc.-Order Model. ROM Simul. Optim., 1st ed., Springer International Publishing, 2018: pp. 167–179.
[25] D.S. Alves, G.B. Daniel, H.F. de Castro, T.H. Machado, K.L. Cavalca, O. Gecgel, J.P. Dias, S. Ekwaro-Osire, Uncertainty quantification in deep convolutional neural network diagnostics of journal bearings with ovalization fault, Mech. Mach. Theory. 149 (2020) 103835, doi:10.1016/j.mechmachtheory.2020.103835.
[26] W.L. Chan, M.W. Fu, J. Lu, An integrated FEM and ANN methodology for metal-formed product design, Eng. Appl. Artif. Intell. 21 (2008) 1170–1181, doi:10.1016/j.engappai.2008.04.001.
[27] P. Dong, S. Zuo, S. Du, P. Tenberge, S. Wang, X. Xu, X. Wang, Optimum design of the tooth root profile for improving bending capacity, Mech. Mach. Theory. 151 (2020) 103910, doi:10.1016/j.mechmachtheory.2020.103910.
[28] G. Bonori, M. Barbieri, F. Pellicano, Optimum profile modifications of spur gears by means of genetic algorithms, J. Sound Vib. 313 (2008) 603–616, doi:10.1016/j.jsv.2007.12.013.
[29] S. Chavadaki, K.C. Nithin Kumar, M.N. Rajesh, Finite element analysis of spur gear to find out the optimum root radius, Mater. Today Proc. (2021), doi:10.1016/j.matpr.2021.01.422.
[30] R. He, P. Tenberge, X. Xu, H. Li, R. Uelpenich, P. Dong, S. Wang, Study on the optimum standard parameters of hob optimization for reducing gear tooth root stress, Mech. Mach. Theory. 156 (2021) 104128, doi:10.1016/j.mechmachtheory.2020.104128.
[31] B. Haefner, M. Biehler, R. Wagner, G. Lanza, Meta-model based on artificial neural networks for tooth root stress analysis of micro-gears, Procedia CIRP 75 (2018) 155–160, doi:10.1016/j.procir.2018.04.031.
[32] H. Chang, P. Borghesani, Z. Peng, Automated assessment of gear wear mechanism and severity using mould images and convolutional neural networks, Tribol. Int. 147 (2020) 106280, doi:10.1016/j.triboint.2020.106280.
[33] W. Li, W. Lin, J. Yu, Predicting contact characteristics for helical gear using support vector machine, Neurocomputing 174 (2016) 1156–1161, doi:10.1016/j.neucom.2015.09.100.
[34] S. Bansal, S. Sahoo, R. Tiwari, D.J. Bordoloi, Multiclass fault diagnosis in gears using support vector machine algorithms based on frequency domain data, Measurement 46 (2013) 3469–3481, doi:10.1016/j.measurement.2013.05.015.
[35] V. Gunasegaran, V. Muralidharan, Fault diagnosis of spur gear system through decision tree algorithm using vibration signal, Mater. Today Proc. 22 (2020) 3232–3239, doi:10.1016/j.matpr.2020.03.283.
[36] X. Li, J. Li, Y. Qu, D. He, Semi-supervised gear fault diagnosis using raw vibration signal based on deep learning, Chin. J. Aeronaut. 33 (2020) 418–426, doi:10.1016/j.cja.2019.04.018.
[37] X. Liu, H. Huang, J. Xiang, A personalized diagnosis method to detect faults in gears using numerical simulation and extreme learning machine, Knowl.-Based Syst. 195 (2020) 105653, doi:10.1016/j.knosys.2020.105653.
[38] S. Xiang, Y. Qin, C. Zhu, Y. Wang, H. Chen, Long short-term memory neural network with weight amplification and its application into gear remaining useful life prediction, Eng. Appl. Artif. Intell. 91 (2020) 103587, doi:10.1016/j.engappai.2020.103587.
[39] H. Yan, Y. Qin, S. Xiang, Y. Wang, H. Chen, Long-term gear life prediction based on ordered neurons LSTM neural networks, Measurement (2020) 108205, doi:10.1016/j.measurement.2020.108205.
[40] A. Kumar, C.P. Gandhi, Y. Zhou, R. Kumar, J. Xiang, Latest developments in gear defect diagnosis and prognosis: a review, Measurement 158 (2020) 107735, doi:10.1016/j.measurement.2020.107735.
[41] Y. Pan, R. Hong, J. Chen, J. Singh, X. Jia, Performance degradation assessment of a wind turbine gearbox based on multi-sensor data fusion, Mech. Mach. Theory. 137 (2019) 509–526, doi:10.1016/j.mechmachtheory.2019.03.036.
[42] U. Urbas, D. Vlah, N. Vukašinović, Machine learning method for predicting the influence of scanning parameters on random measurement error, Meas. Sci. Technol. 32 (2021) 065201, doi:10.1088/1361-6501/abd57a.
[43] J.-.R. Ruiz-Sarmiento, J. Monroy, F.-.A. Moreno, C. Galindo, J.-.M. Bonelo, J. Gonzalez-Jimenez, A predictive model for the maintenance of industrial machinery in the context of industry 4.0, Eng. Appl. Artif. Intell. 87 (2020) 103289, doi:10.1016/j.engappai.2019.103289.
[44] C.M. Bishop, Neural Networks for Pattern Recognition, Oxford University Press, Inc., USA, 1995.
[45] A. Parvaresh, M. Mardani, Data-driven model-free control of torque-applying system for a mechanically closed-loop test rig using neural networks, Stroj. Vestn. - J. Mech. Eng. (2020), doi:10.5545/sv-jme.2019.6499.
[46] Z. Li, Z. Ma, Y. Liu, W. Teng, R. Jiang, Crack fault detection for a gearbox using discrete wavelet transform and an adaptive resonance theory neural network, Stroj. Vestn. - J. Mech. Eng. (2015), doi:10.5545/sv-jme.2014.1769.
[47] C. Guo, L. Chen, J. Ding, A novel dynamics model of ball-screw feed drives based on theoretical derivations and deep learning, Mech. Mach. Theory. 141 (2019) 196–212, doi:10.1016/j.mechmachtheory.2019.07.011.
[48] Y. Zhang, K. Mao, S. Leigh, A. Shah, Z. Chao, G. Ma, A parametric study of 3D printed polymer gears, Int. J. Adv. Manuf. Technol. 107 (2020) 4481–4492, doi:10.1007/s00170-020-05270-5.
[49] J. Dekhtiar, A. Durupt, M. Bricogne, B. Eynard, H. Rowson, D. Kiritsis, Deep learning for big data applications in CAD and PLM – Research review, opportunities and case study, Comput. Ind. 100 (2018) 227–243, doi:10.1016/j.compind.2018.04.005.
[50] M. Bramer, Principles of Data Mining, 3rd ed., Springer-Verlag, London, 2016.
[51] T. Hastie, R. Tibshirani, J. Friedman, The Elements of Statistical Learning: Data Mining, Inference, and Prediction, second ed., Springer, 2009.
[52] M. Cerrada, G. Zurita, D. Cabrera, R.-.V. Sánchez, M. Artés, C. Li, Fault diagnosis in spur gears based on genetic algorithm and random forest, Mech. Syst. Signal Process. 70–71 (2016) 87–103, doi:10.1016/j.ymssp.2015.08.030.
[53] C. Xiao, N. Chen, C. Hu, K. Wang, J. Gong, Z. Chen, Short and mid-term sea surface temperature prediction using time-series satellite data and LSTM-AdaBoost combination approach, Remote Sens. Environ. 233 (2019) 111358, doi:10.1016/j.rse.2019.111358.
[54] D.J. Bordoloi, R. Tiwari, Optimum multi-fault classification of gears with integration of evolutionary and SVM algorithms, Mech. Mach. Theory. 73 (2014) 49–60, doi:10.1016/j.mechmachtheory.2013.10.006.
[55] D. Wang, K-nearest neighbors based methods for identification of different gear crack levels under different motor speeds and loads: revisited, Mech. Syst. Signal Process. 70–71 (2016) 201–208, doi:10.1016/j.ymssp.2015.10.007.
[56] J. Hlebanja, G. Hlebanja, Constructive measures to increase the load-carrying capacity of gears: the characteristics of S-gears, Mach. Des. 1 (2008).
[57] A. Artoni, A methodology for simulation-based, multiobjective gear design optimization, Mech. Mach. Theory. 133 (2019) 95–111, doi:10.1016/j.mechmachtheory.2018.11.013.
[58] A. Bravo, L. Toubal, D. Koffi, F. Erchiqui, Gear fatigue life and thermomechanical behavior of novel green and bio-composite materials VS high-performance thermoplastics, Polym. Test. 66 (2018) 403–414, doi:10.1016/j.polymertesting.2016.12.031.
[59] J. Tavčar, B. Černe, J. Duhovnik, D. Zorko, A multicriteria function for polymer gear design optimization, J. Comput. Des. Eng. (2021), doi:10.1093/jcde/qwaa097.
[60] Simon Kulovec, Jože Duhovnik, Variation of S-gear shape and the influence of the main parameters, in: proc. Int. Conf. Gears 2013, Garching, 2013: pp. 1535–1541.
[61] B. Černe, R. Lorber, J. Duhovnik, J. Tavčar, Influence of temperature- and strain rate-dependent viscoplastic properties of polyoxymethylene on the thermo-mechanical response of a steel-polyoxymethylene spur gear pair, Mater. Today Commun. 25 (2020) 101078, doi:10.1016/j.mtcomm.2020.101078.
[62] Damijan Zorko, Jože Duhovnik, Jože Tavčar, Tooth bending strength of gears with a progressive curved path of contact, Journal of Computational Design and Engineering 8 (2021) 1037–1058, doi:10.1093/jcde/qwab031.